Journal of
Materials Chemistry C

Accepted Manuscript

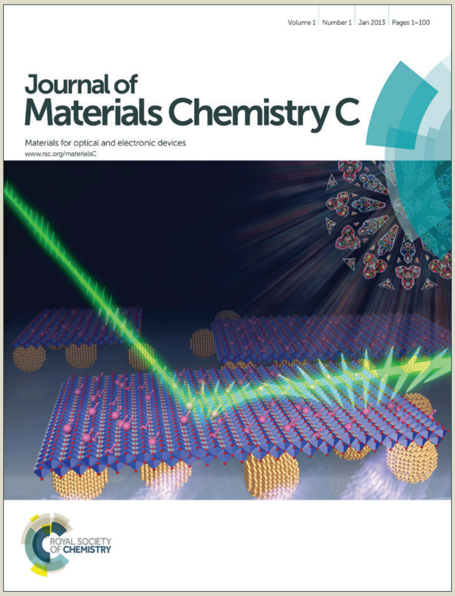

ROYAL SOCIETY
OF CHEMISTRY

www.rsc.org/materialsC

A highly selective fluorescent sensor for Zn^{2+} and Cu^{2+} based on a diarylethene with a piperazine-linked amidoquinoline unit

Shuijun Xia, Gang Liu, Shouzhi Pu*

Jiangxi Key Laboratory of Organic Chemistry, Jiangxi Science and Technology Normal University,

Nanchang 330013, PR China

***Corresponding author:** E-mail address: pushouzhi@tsinghua.org.cn (S. Pu); Tel./Fax: +86-791-83831996.

Abstract: A novel asymmetrical diarylethene with a piperazine-linked amidoquinoline unit was synthesized and its multi-controllable switching behaviors induced by light and chemical stimuli were investigated in detail. The diarylethene was highly selective towards Zn^{2+} and Cu^{2+} with different fluorescence signals and binding modes. When triggered by Zn^{2+}, its fluorescence intensity was enhanced evidently and its emission peak was red-shifted from 417 nm to 502 nm with a concomitant color change from light blue to bright green. In contrast, its fluorescence intensity notably decreased accompanied with a color change from light blue to dark when stimulated by Cu^{2+}. The binding affinity of the diarylethene to Cu^{2+} (irreversible) was much higher than that to Zn^{2+} (reversible) with a binding stoichiometry of 1:1 to both ions. In addition, its light and metal-responsive fluorescence behavior was applied to the construction of a molecular logic circuit with four inputs and one output.

Keywords: Photochromism; Diarylethene; Piperazine-linked amidoquinoline; Ion recognition; Fluorescence switch; Logic circuit.

Introduction

Molecular fluorescent probes have received immense interest due to their huge potential in chemical, environmental, and biological applications.[1-7] In particular, the development of a fluorescent probe to the detection of metal ions has received much attention. Zinc ion plays an important role in gene expression, neural signal transmission, immune functions, and various other fundamental biological processes.[8,9] Elevated level of Zn^{2+} in humans has been implicated in neurodegenerative disorders.[10,11] In recent years, great efforts have been devoted to the design and synthesis of Zn^{2+}-selective in vitro and/or in vivo fluorescent sensors.[12-16] Meanwhile, because copper ion plays an important role in human body and is a widespread metal pollutant,[17,18] much attention has been paid to the development of effective fluorescent Cu^{2+} probes in biological and environmental systems.[19-22] However, fluorescent probes for both Zn^{2+} and Cu^{2+} are rarely reported.[23-26]

Photochromic materials have attracted much attention in recent years because of their potential applications in optical information storage media and photonic switch devices.[27,28] Among various photochromic compounds, diarylethenes (DAEs) are one of the most promising photoswitchable molecules because their isomers are thermally stable and fatigue-resistant.[29,30] Furthermore, their fluorescence can be reversibly modulated by alternating irradiation with UV and visible light. So far, many DAEs fluorescence chemosensors with various functional groups have been designed and synthesized.[31-36] However, photochromic diarylethene-based fluorescent chemosensors for Zn^{2+} and Cu^{2+} have rarely been reported. On the other hand, quinoline derivatives are ideal probes for Zn^{2+} because of their good photostability, strong binding ability, and convenient synthesis.[37,38] Meanwhile, the flexible conformation of the piperazine favors a tunable and suitable coordination structure.[39,40]

On the basis of the mentioned facts, we constructed a highly selective fluorescent chemosensor for Zn^{2+}

and Cu^{2+} by using a new photochromic diarylethene with a piperazine-linked amidoquinoline unit (**Fig. 1**). Furthermore, a logic circuit was generated based on the unimolecular platform by employing fluorescence mode at 502 nm wavelength as the output and appropriate combination of chemical and light stimuli as inputs.

<Fig. 1>

Experimental

General methods

Unless otherwise stated, all of the materials for the synthesis of **1O** were purchased from various commercial sources and used without further purification. Solvents used were purified by standard methods prior to use. The solutions of metal ions (0.1 mol L^{-1}) were prepared by the dissolution of their respective metal nitrates in distilled water, except for Mn^{2+}, Hg^{2+}, K^{+}, and Ba^{2+} (all of their counter ions were chloride ions). NMR spectra were recorded on a BRUKER AV400 spectrometer by using TMS as an internal standard and with $CDCl_3$ as the solvent. Mass spectra were performed using an Agilent 1100 ion trap MSD spectrometer. Melting point was obtained on a WRS-1B melting point apparatus. Fluorescence spectra were recorded with a HITACHI F4600 fluorescence spectrophotometer with the excitation and emission slit widths at 5.0 and 5.0 nm, respectively. UV−vis spectra were measured on an Agilent 8453 UV−vis spectrophotometer. Infrared spectra (IR) were collected on a Bruker Vertex-70 spectrometer. Elemental analysis was carried out with a PE CHN 2400 analyzer. Fluorescence quantum yield was measured with Absolute PL Quantum Yield Spectrometer QY C11347-11.

Synthesis

The synthetic route to the target diarylethene, 1-(2-methyl-3-benzothiophenyl)-2-{2-methyl-5-[4-N-(quinol-8-yl)acetaminepiperazine-methylphenyl]-3-thienyl}perfluorocyclopentene (**1O**), is shown in

Fig. 2. The intermediate products **2–4** were synthesized according to the procedures of reported methods.[41,42]

<Fig. 2>

*N-(quinol-8-yl)acetaminepiperazine (**5**)*

The piperazine (110 mg, 1.2 mmol), and K_2CO_3 (1.4 g, 10 mmol) were dissolved in anhydrous CH_3OH (5 mL), and compound **4** (220 mg, 1.0 mmol) was added dropwise under vigorous stirring. The mixture was refluxing for 6 h under a nitrogen atmosphere, and then cooled to room temperature. The crude product was purified by extracting, evaporating, and separating on a silica gel chromatography column with dichloromethane/methanol (10:1) as the eluent to afford 0.1 g of **5** as a yellow liquid in 30 % yield. ^{1}H NMR (400 MHz, $CDCl_3$) δ 11.48 (s, 1H), 8.88–8.90 (m, 1H), 8.77–8.79 (m, 1H), 8.16–8.18 (m, 1H), 7.59–7.52 (m, 2H), 7.46–7.50 (m, 1H), 3.40 (s, 2H), 2.92 (s, 4H), 2.65(s, 4H). ^{13}C NMR ($CDCl_3$, 100 MHz): 38.5, 40.1, 53.1, 53.2 62.50, 116.5, 121.6,127.2,128.8, 129.2, 134.3, 136.1, 139.0, 148.6, 169.0. LRMS (ESI$^+$): *m/z* 271.2 $[M + H]^+$.

*1-(2-Methyl-3-benzothiophenyl)-2-{2-methyl-5-[4-N-(quinol-8-yl)acetaminepiperazine-methylphenyl]-3-thienyl} perfluorocyclopentene (**1O**)*

A mixture of compound **3** (176 mg, 0.3mmol), **5** (660mg, 3 mmol), K_2CO_3 (413 mg, 3 mmol), and KI (50 mg, 0.3 mmol) in anhydrous CH_3CN (5 mL) was stirred at 80 °C for 6 hours under a nitrogen atmosphere. The reaction mixture was cooled and solvent was removed under reduced pressure, extracted with diethyl ether. The organic layer was washed with water, dried over anhydrous Na_2SO_4, and evaporated. The crude product was purified by column chromatography using dichloromethane/methanol (30:1) as the eluent to obtain 0.30 g of the target compound **1O** as a purple solid in 55% yield. M.p. 405–406 K; δ^{1}H NMR (400 MHz, $CDCl_3$) δ 11.43 (s, 1H), 8.80–8.82 (m, 1H), 8.68–8.80 (m, 1H), 8.23–8.25 (m, 1H), 7.81 (d, J = 7.2 Hz, 1H), 7.60–7.53 (m, 1H), 7.47–7.49 (m, 1H), 7.43 (d, J = 8.3 Hz, 1H), 7.39–7.30 (m, 1H), 7.23 (s, 1H), 3.60 (s, 1H), 3.23 (s, 1H), 2.68 (s, 1H), 2.63 (s, 1H), 2.38 (s, 1H), 2.01 (s, 1H). ^{13}C NMR ($CDCl_3$, 100 MHz): 14.9, 15.4, 55.0, 55.2, 63.5, 64.3, 118.5, 120.3, 121.5, 122.1, 122.4, 123.5, 124.7, 125.0, 125.3, 125.6, 126.5, 127.2, 127.2, 127.3, 127.8, 127.65, 128.26, 128.4, 128.6, 132.3, 134.1, 136.6, 136.7, 136.9, 137.5, 137.9, 139.3, 148.8, 168.5. IR (KBr, cm): 759, 788, 992, 1105, 1132, 1271, 1423, 1517, 1686, 2818. LRMS (ESI$^+$): *m/z* 777.1 $[M + H]^+$; Anal. Calcd. for $C_{41}H_{34}F_6N_4OS_2$ (%): C, 63.08; H, 4.30; N, 7.49, found: C, 63.39; H, 4.41; N, 7.41.

Results and discussion

Photochromism and fluorescence of 1O

The photochromic and fluorescent properties of **1O** were studied in THF solution (2.0×10^{-5} mol L^{-1}) at room temperature. As shown in **Fig. 3A**, diarylethene **1O** was colorless with a sharp absorption peak at 300 nm in THF. When irradiated with 297 UV light, a new absorption band centered at 550 nm appeared and the color changed to purple due to the photocyclization reaction of **1O** to **1C**.[43] After irradiation with UV light for 5 min, the photocyclization reaction reached a photostationary state (PSS) and a clear isosbestic point was observed at 307 nm. The quantum yields of the cyclization and cycloreversion of **1** were determined to be 0.40 and 0.041, respectively. When the solution at PSS was irradiated with appropriate visible light (λ > 450 nm), the purple solution turned colorless and its absorption spectrum was recovered to that of the open-ring isomer **1O**. The coloration–decoloration cycles could be repeated for 10 times with a negligible degradation. Impressively, both of the two isomers of **1** showed excellent thermal stability when stored in THF at 338 K in the dark for more than 6 days. **Fig. 3B** showed that the fluorescence spectral change of **1O** in THF upon photoirradiation. When excited at 340 nm, weak fluorescence centered at 417 nm can be seen and the fluorescence quantum yield was determined to be

0.009. Upon irradiation with 297 nm UV light, distinct fluorescence quenching was observed along with the occurring of photocyclization reaction. When arrived at PSS, the fluorescence intensity of **1O** was quenched to *ca.* 30% due to the formation of the non-fluorescent closed-ring isomer **1C**.[44,45] Reversely, the fluorescence of **1O** could be restored by irradiation with appropriate visible light (λ > 550 nm).

<Fig. 3>

Fluorescence response to metal ions

<Fig. 4>

<Fig. 5>

The binding ability of **1O** with various metal cations including K^+, Ca^{2+}, Ba^{2+}, Pb^{2+}, Mg^{2+}, Sr^{2+}, Al^{3+}, Fe^{3+}, Cr^{3+}, Cu^{2+}, Ni^{2+}, Co^{2+}, Hg^{2+}, Mn^{2+}, Cd^{2+}, and Zn^{2+} were investigated by fluorescence spectroscopy. **Fig. 4** shows the emission spectrum and fluorescence color change of **1O** in THF (2.0×10^{-5} mol L^{-1}) induced by the addition of metal ions (1.0 equiv). It could be seen that the fluorescence of **1O** was notably changed only when Zn^{2+} or Cu^{2+} was added. The addition of other cations, such as K^+, Ca^{2+}, Ba^{2+}, Pb^{2+}, Mg^{2+}, Sr^{2+}, Al^{3+}, Fe^{3+}, Cr^{3+}, Ni^{2+}, Fe^{3+}, Co^{2+}, Hg^{2+}, Mn^{2+}, and Cd^{2+}, resulted in no obvious change in the fluorescence of **1O**. When Zn^{2+} was added to the solution of **1O**, the fluorescence intensity was enhanced evidently and the emission peak red-shifted from 417 nm to 502 nm with a concomitant color change from light blue to bright green. The redshift of 85 nm could be ascribed to the formation of a complex of **1O-Zn^{2+}**.[46] In contrast, the fluorescence intensity of **1O** dramatically decreased with a minor redshift of the emission peak from 417 nm to 443 nm and a color change from light blue to dark, when Cu^{2+} was applied. As a result, the diarylethene could be used as a selective fluorescence sensor for Zn^{2+} and Cu^{2+} ions over other competing metal ions in THF. Furthermore, the fluorescence quantum yields of **1O-Zn^{2+}** and **1O-Cu^{2+}** were determined to be 0.024 and 0.003, respectively. In addition, the complex **1O-Zn^{2+}** also functioned as a notable fluorescence switch upon irradiation with UV/vis light. When reached the photostationary state, the emission intensity was quenched to *ca.* 27% due to the formation of **1C-Zn^{2+}** complex (**Fig. 5A**). The complex **1O-Cu^{2+}** (colorless) turned to **1C-Cu^{2+}** (purple) upon irradiation with UV light, but its fluorescence exhibited no obvious change due to the relatively weak fluorescence. Moreover, to examine whether the coordinating processes of **1O** with Zn^{2+} and Cu^{2+} were reversible or not, 12 equiv of EDTA (0.1 mol L^{-1}) was added to the solutions of **1O-Zn^{2+}** and **1O-Cu^{2+}**, respectively. The results showed that the fluorescence spectrum of **1O-Zn^{2+}** recovered immediately to that of **1O** (**Fig. 5B**), indicating that the complexation/decomplexation reaction between **1O** and Zn^{2+} was reversible. However, the fluorescence spectrum of **1O-Cu^{2+}** could not be restored to that of **1O** even excess amount of EDTA solution had been added, indicating that the complexation/decomplexation reaction between **1O** and Cu^{2+} was irreversible.

<Fig. 6>

In addition, a competitive experiment was performed by titrating Cu^{2+} into a solution of the **1O-Zn^{2+}**. The fluorescence changes of **1O** induced by adding Zn^{2+} are shown in **Fig. 6**. As shown in **Fig. 6A**, the **1O-Zn^{2+}** complex was formed by adding 2.5 equiv of Zn^{2+} into the solution of **1O** (2.0×10^{-5} mol L^{-1}). Then, titrating 1.0 equiv of Cu^{2+} into the solution of **1O-Zn^{2+}** resulted in a notable fluorescence intensity decrease with a concomitant color change from bright green to dark (**Fig. 6B**). The fluorescence profile upon titration of **1O-Zn^{2+}** with Cu^{2+} was the same as that of **1O-Cu^{2+}**, indicating that the Zn^{2+} in **1O-Zn^{2+}** complex was replaced by Cu^{2+} and the **1O-Cu^{2+}** complex was produced. A reverse competitive test confirmed that the **1O-Zn^{2+}** complex could not form upon the titration of **1O-Cu^{2+}** complex with Zn^{2+}. The results elucidated that **1O** bound to Cu^{2+} much more tightly than to Zn^{2+}.

<Fig. 7>

To further evaluate the affinities between **1O** and Zn^{2+}/Cu^{2+}, a series of tests including fluorescence titration, Job's plot, ^{1}H NMR spectroscopy, and mass spectroscopy were performed. The results of fluorescence changes by titrating Zn^{2+} and Cu^{2+} into the solution of **1O** are shown in **Fig. 7**. The gradually increased Zn^{2+}concentration (0-2.5 equiv) resulted in a fluorescence enhancement up to 2 fold around 502 nm due to a typical of ICT-based optical response (**Fig. 7A**). Upon the gradual addition of Cu^{2+} (0-1.0 equiv) to the solution of **1O**, the fluorescence intensity at 417 nm was dramatically quenched (**Fig. 7B**). This quenching of fluorescence intensity of **1O** induced by Cu^{2+} ion may be attributed to the paramagnetic nature of Cu^{2+}.[47] Moreover, linear relationships were obtained from the fluorescence titration profiles for the plots measured at 502 nm for **1O**-Zn^{2+} and 417 nm for **1O**-Cu^{2+} as a function of $1/[M^{2+}]$ using the linear Benesi−Hildebrand expression and Stern−Volmer plot. Obtained from the slope and intercept of these linear plots, the association constants (K_a) of **1O** with Zn^{2+} and Cu^{2+} were found to be 7.8×10^5 (R = 0.995) and 1.55×10^6 L mol^{-1} (R = 0.993), respectively. These results further confirmed that **1O** bound to Cu^{2+} with a higher affinity. The detection limits were calculated to be 5.5×10^{-5} mol L^{-1} for Zn^{2+} and 2.7×10^{-5} mol L^{-1} for Cu^{2+} by the reported method.[48] To determine the interaction stoichiometry between **1O** and Zn^{2+}/Cu^{2+}, Job's plots were obtained by using an intensity at 502 nm for Zn^{2+} and 417 nm for Cu^{2+} as a function of molar fraction of **1O** (**Fig. S1**). The maximum fluorescence of **1O**-Zn^{2+} and the minimum value of **1O**-Cu^{2+} were observed when the molar fraction of **1O** was 0.50, indicating that **1O** bound to Zn^{2+} and Cu^{2+} with a binding stoichiometry of 1:1.

<Fig. 8>

In order to confirm the selectivity of **1O** as a fluorescence sensor for Zn^{2+} and Cu^{2+}, the effects of competing metal ions were studied. As shown in **Fig. 8**, no obvious interference in its fluorescence was observed when Zn^{2+} (2.5 equiv) was added to the solutions containing **1O** and the same amount of other metal ions except Cu^{2+}. No evident variations in fluorescence intensity were found in comparison with that with Zn^{2+} alone. Upon the further addition of Cu^{2+} (1.0 equiv) to the solutions of **1O**-Zn^{2+} containing other competitive metal ions, their fluorescence intensities were all decreased even if the amount of other metal ions was larger than that of Cu^{2+}. The results revealed that Cu^{2+} had a significant effect on the fluorescence of **1O**-Zn^{2+} and the Cu^{2+}-specific response was not disturbed by other competitive metal ions.

Fig. S2 shows the ^{1}H NMR spectra of **1O**, **1O-Zn^{2+}**, and **1O-Cu^{2+}** in DMSO-d_6 and $CDCl_3$. The protons of **1O** displayed a signal at 3.24 ppm for one methylene group (proton-*a*), 3.58 ppm for the other methylene group (proton-*b*), and 2.61-2.66 ppm for the piperazine unit (protons-*c*). After complexation with Zn^{2+}, the peak of proton-*b* became broadened and shifted to downfield at 3.60 ppm, which was assigned to the formation of Zn^{2+}-N and Zn^{2+}-O interactions. However, there was no shift at the positions proton-*a* and -*c*. When 1.0 equiv of Cu^{2+} was added to the **1O-Zn^{2+}** solution, the signals of proton-*a* and -*b* were gradually covered by that of the solvent peak. At the same time, the peak of proton- *c* became smooth, which might be ascribed to the paramagnetic property of Cu^{2+}. In addition, the 1:1 binding stoichiometry was further confirmed by the ESI-MS method. As shown in **Fig. S3**, the free **1O** had a main peak at *m/z* 777.1 for [**1O-H**]$^+$. When excess amounts of Zn^{2+} was added to **1O**, the peak at *m/z* 777.1 disappeared and a new peak at *m/z* 966.5 appeared due to the formation of [**1O-Zn(NO$_3$)$_2$+H**]$^-$. When excess amount of Cu^{2+} was added to **1O-Zn^{2+}**, a new peak at *m/z* 838.0 showed up due to the formation of [**1O-Cu^{2+}-H**]$^+$.

Application as a logic circuit

Generally, molecules interplaying with various kinds of inputs have been applied in the construction of molecular logic gates and circuits.[49,50] On the basis of the fact that the fluorescence intensity of **1O** could be notably modulated by the stimulation of light and chemical species, a molecular logic gate was constructed by four inputs (UV, Cu^{2+}, Zn^{2+}, and EDTA) and one output (fluorescence intensity at 502 nm). The four inputs were represented as I1, I2, I3, and I4, respectively, and they could be either ‘on’ or ‘off’ states with different Boolean values. For example, input signal I1 was switched to ‘on’ state with a Boolean value ‘1’, when 297 nm UV irradiation was employed. Similarly, input I2 was ‘1’ corresponding to the addition of Cu^{2+}, I3 was ‘1’ corresponding to the addition of Zn^{2+}, and I4 was ‘1’ corresponding to the addition of EDTA. Diarylethene **1O** exhibited strong fluorescence induced by the stimulation of Zn^{2+}, and its fluorescence intensity was used as an initial state. The output signal could serve as ‘on’, when the fluorescence intensity at 502 nm was 50% higher than the initial value. Otherwise, it was regarded as ‘off’. As a result, **1O** can read a string of four inputs and write one output. Concretely, if the string is ‘0, 0, 1, and 0’ , its corresponding inputs I1, I2, I3, and I4 are ‘off, off, on, and off’, respectively. Diarylethene **1O** was converted to **1O-Zn^{2+}** and its fluorescence was enhanced, resulting in the ‘on’ state of the output signal. All the possible strings of the four inputs were listed in **Table 1**, and the logic circuit corresponding to the truth table is presented in **Fig. 9**.

<Table 1>

<Fig. 9>

Conclusion

In summary, a novel asymmetrical diarylethene has been synthesized by using perfluorocyclopentene diarylethene as a photoswitchable core and amidoquinoline as a multi-responsive group via a piperazine linkage. Our experimental results demonstrated that the diarylethene **1** could readily recognize Zn^{2+} and Cu^{2+} with remarkably different fluorescence signals and had distinct binding modes to Zn^{2+} and Cu^{2+}. Based on the fact that the fluorescence of the diarylethene could be effectively modulated by the stimulation of light and chemical species, a multi-controllable switch and an integrated logic circuit was successfully designed and constructed. This work provides a new approach for the design and construction of fluorescent sensors based on photochromic diarylethenes with multi-controllable switching behaviors and different selectivity for multiple targets of interest.

Acknowledgements

The authors are grateful for the financial support from the National Natural Science Foundation of China (21162011, 21262015, 51373072), the Project of Jiangxi Advantage Sci-Tech Innovative Team (20142BCB24012), the Science Funds of Natural Science Foundation of Jiangxi Province (20132BAB203005), and the Project of the Science Funds of Jiangxi Education Office (KJLD13069, KJLD12035, GJJ12587).

References

1. E. L. Que, D. W. Domaille and C. J. Chang, *Chem. Rev.*, 2008, **108**, 1517-1549.
2. X.M. Liu, N. Xi, S.J. Liu, Y. Ma, H.R. Yang, J.H. Li, J. He, Q. Zhao, F.Y. Li and W. Huang, *J. Mater. Chem.*, 2012, **22**, 7894-7901.
3. Y. Ma, S.J. Liu, H.R. Yang, Y.Q. Wu, C.J. Yang, X.M. Liu, Q. Zhao, H.Z. Wu, J.C. Liang, F.Y. Li and W. Huang, *J. Mater. Chem.*, 2011, **21**, 18974-18982.
4. H.F. Shi, H.B. Sun, H.R. Yang, S.J. Liu, G. Jenkins, W. Feng, F.Y. Li, Q. Zhao, B. Liu and W. Huang, *Adv. Funct. Mater.*, 2013, **23**, 3268-3276.
5. W.J Xu, S.J. Liu, H.B. Sun, X.Y. Zhao, Q. Zhao, S. Sun, S. Cheng, T.C. Ma, L. Zhou and W. Huang, *J. Mater. Chem.*, 2011, **21**, 7572-7581.
6. K. Y. Zhang, J. Zhang, Y.H. Liu, S.J. Liu, P.L. Zhang, Q. Zhao, Y. Tang and W. Huang, *Chem. Sci.*, 2015, **6**, 301-307

7. Q. Zhao, X.B. Zhou, T.Y. Cao, K. Y. Zhang, L.J Yang, S. Liu, H. Liang, H. Yang, F.Y. Li and W. Huang, *Chem. Sci.*, 2015, **6**, 1825-1831.

8. Z. Dai and J. W. Canary, *New J. Chem.*, 2007, **31**, 1708-1718.

9. L. Xu, Y.F. Xu, W.P. Zhu, B.B. Zeng, C. Yang,M. B. Wu and X.H. Qian, *Org. Biomol. Chem.*, 2011, **9**, 8284-8287.

10. Z.C. Xu, K.-H. Baek, H. N. Kim, J.N. Cui, X.H. Qian, D. R. Spring, I. Shin and J. Yoon, *J. Am. Chem. Soc.*, 2009, **132**, 601-610.

11. P.W. Du and S. J. Lippard, *Inorg. Chem.*, 2010, **49**, 10753-10755.

12. Z.X. Li, M.M. Yu, L.F. Zhang, M. Yu, J. Liu, L.H. Wei and H.Y. Zhang, *Chem. Commun.*, 2010, **46**, 7169-7171.

13. S. Y. Assaf and S.-H. Chung, *Nature*, 1984, **308**, 734-736.

14. E. Tamanini, K. Flavin, M. Motevalli, S. Piperno, L. A. Gheber, M. H. Todd and M. Watkinson, *Inorg. Chem.*, 2010, **49**, 3789-3800.

15 X. Lu, W. Zhu, Y. Xie, X. Li, Y. Gao, F. Li and H. Tian, *Chem. –Eur. J.*, 2010, **16**, 8355-8364.

16. C. Frederickson and A. Bush, *Biometals*, 2001, **14**, 353-366.

17. D. T. Quang and J. S. Kim, *Chem. Rev.*, 2010, **110**, 6280-6301.

18. K. Rurack, *Spectrochim. Acta A*, 2001, **57**, 2161-3195.

19. R. Krämer, *Angew. Chem. Int. Ed.*, 1998, **37**, 772-773.

20. G. Multhaup, A. Schlicksupp, L. Hesse, D. Beher, T. Ruppert, C. L. Masters and K. Beyreuther, *Science*, 1996, **271**, 1406-1409.

21. R. Løvstad, *Biometals*, 2004, **17**, 111-113.

22. D. W. Domaille, L. Zeng and C. J. Chang, *J. Am. Chem. Soc.*, 2010, **132**, 1194-1195.

23. Z.X. Li, L.F. Zhang, L. Wang, Y.K. Guo, L.H. Cai, M.M. Yu and L.H. Wei, *Chem. Commun.*, 2011, **47**, 5798-5800.
24. M.-M. Yu, Z.-X. Li, L.-H. Wei, D.-H. Wei and M.-S. Tang, *Org. Lett.*, 2008, **10**, 5115-5118.
25. D. Sarkar, A. K. Pramanik and T. K. Mondal, *RSC Adv.*, 2014, **5**, 7647-7653.
26. S. Anbu, R. Ravishankaran, M. F. Guedes da Silva, A. A. Karande and A. J. Pombeiro, *Inorg. Chem.*, 2014, **53**, 6655-6664.
27. H. Dürr and H. Bouas-Laurent, *Photochromism: Molecules and Systems*, Elsevier, Amsterdam, 1990.
28. B. L. Feringa, *Molecular Switches*, Wiley-VCH, Weinheim, 2001.
29. H. Tian and S. Yang, *Chem. Soc. Rev.*, 2004, **33**, 85-97.
30. M. Irie, *Chem. Rev.*, 2000, **100**, 1685-1716.
31. L. Giordano, T. M. Jovin, M. Irie and E. A. Jares-Erijman, *J. Am. Chem. Soc.*, 2002, **124**, 7481-7489.
32. H.C. Ding, G. Liu, S.Z. Pu and C.H. Zheng, *Dyes Pigm.*, 2014, **103**, 82-88.
33. S.Z. Pu, H.C. Ding, G. Liu, C.H. Zheng and H.Y. Xu, *J. Phys. Chem. C*, 2014, **118**, 7010-7017.
34. T. Fukaminato, T. Doi, N. Tamaoki, K. Okuno, Y. Ishibashi, H. Miyasaka and M. Irie, *J. Am. Chem. Soc.*, 2011, **133**, 4984-4990.
35. Q. Zou, X. Li, J. Zhang, J. Zhou, B. Sun and H. Tian, *Chem. Commun.*, 2012, **48**, 2095-2097.
36. J. He, J. He, T. Wang and H. Zeng, *J. Mater. Chem. C*, 2014, **2**, 7531-7540.
37. P. Jiang and Z. Guo, *Coord. Chem. Rev.*, 2004, **248**, 205-229.
38. M. Rouffet, C. A. F. de Oliveira, Y. Udi, A. Agrawal, I. Sagi, J. A. McCammon and S. M. Cohen, *J. Am. Chem. Soc.*, 2010, **132**, 8232-8233.

39. J. Jiang, H. Jiang, X. Tang, L. Yang, W. Dou, W. Liu, R. Fang and W. Liu, *Dalton. Trans.*, 2011, **40**, 6367-6370.

40. J. Zhang, W. Tan, X. Meng and H. Tian, *J. Mater. Chem.* 2009, **19**, 5726-5729.

41. X.W. Cao, W.Y. Lin and L.W. He, *Org. Lett.*, 2011, **10**, 4716-4719.

42. S.Z. Pu, L.L. Ma, G. Liu, H.C. Ding and B. Chen, *Dyes Pigm.*, 2015, **113**, 70-77.

43. G. Liu, S.Z. Pu and X. Wang, *J. Photochem. Photobiol., A: Chem.*, 2010, **214**, 230-240.

44. T. Fukaminato, T. Sasaki, T. Kawai, N. Tamai and M. Irie, *J. Am. Chem. Soc.*, 2004, **126**, 14843-14849.

45. T. Kawai, T. Sasaki and M. Irie, *Chem. Commun.*, 2001, 711-712.

46. X. Zhou, P. Li, Z. Shi, X. Tang, C. Chen and W. Liu, *Inorg. Chem.*, 2012, **51**, 9226-9231.

47. H. S. Jung, P. S. Kwon, J. W. Lee, J. I. Kim, C. S. Hong, J. W. Kim, S. Yan, J. Y. Lee, J. H. Lee, T. Joo and J. S. Kim, *J. Am. Chem. Soc.*, 2009, **131**, 2008-2012.

48. S. Tao, Y. Wei, C. Wang, Z. Wang, P. Fan, D. Shi, B. Ding and J. Qiu, *RSC Adv.*, 2014, **4**, 46955-46961.

49. H. Tian, *Angew. Chem. Int. Ed.*, 2010, **49**, 4710-4712.

50. Y. Wu, Y. Xie, Q. Zhang, H. Tian, W. Zhu and A. D. Q. Li, *Angew. Chem.*, 2014, **126**, 2122-2126.

Table 1. Truth table of all possible strings with four binary-input data and the corresponding output digit.

Input-1 (UV)	Input-2 (Cu^{2+})	Input-3 (Zn^{2+})	Input-4 (EDTA)	Output (502 nm)
0	0	0	0	0
0	1	0	0	0
0	0	1	0	1
0	0	0	1	0
0	1	1	0	0
0	0	1	1	0
0	1	0	1	0
0	1	1	1	0
1	0	0	0	0
1	0	0	1	0
1	0	1	0	0
1	1	0	0	0
1	0	0	1	0
1	1	1	0	0
1	0	1	1	0
1	1	1	1	0

Figure Captions:

Fig. 1. Photochromism of diarylethene **1**.

Fig. 2. Synthetic route to diarylethene **1O**.

Fig. 3. Absorption and emission spectral changes of **1O** in THF (2.0×10^{-5} mol L^{-1}): (A) absorption spectral change, (B) emission spectral change, excited at 340 nm.

Fig. 4. Changes in the fluorescence of **1O** induced by the addition of various metal ions (2.5 equiv) in THF (2.0×10^{-5} mol L^{-1}): (A) emission spectral changes, (B) photographs of the color changes in fluorescence.

Fig. 5. Changes in the fluorescence of **1O-Zn^{2+}** induced by the stimulation of UV/vis irradiation and EDTA/Zn^{2+} in THF (2.0×10^{-5} mol L^{-1}): (A) UV/vis irradiation, (B) EDTA/Zn^{2+}.

Fig. 6. Change in the fluorescence of **1O** induced by the stimulation of Zn^{2+} and/or Cu^{2+} in THF (2.0×10^{-5} mol L^{-1}): (A) emission spectral changes (2.5 equiv of Zn^{2+} ion and 1.0 equiv of Cu^{2+} were used, excited at 340 nm), (B) photographs of the color changes in fluorescence.

Fig. 7. Changes in the fluorescence of **1O** with the concentration changes of Zn^{2+} and Cu^{2+} in THF (2.0×10^{-5} mol L^{-1}): (A) Zn^{2+}, (B) Cu^{2+}. Insets show the Benesi−Hildebrand (A) and Stern−Volmer (B) plots.

Fig. 8. Competitive tests for the fluorescence responses of **1O-Zn^{2+}** to various metal ions in THF (2.0×10^{-5} mol L^{-1}), excited at 340 nm. Bars represent the emission intensity at 502 nm. The gray bars represent the emission intensity of **1O** induced by the addition of 2.5 equiv of various metal ions. The red bars represent the emission intensity of metal ion-contained solution followed by the addition of 2.5 equiv of Zn^{2+}. The blue and the green bars represent the addition of Cu^{2+} (2.5 equiv) and Zn^{2+} (2.5 equiv) to the above solution, respectively.

Fig. 9. The combinational logic circuits equivalent to the truth table given in Table 1: I1 (297 nm UV

light), I2 (Zn^{2+}), I3 (Cu^{2+}), I4 (EDTA).

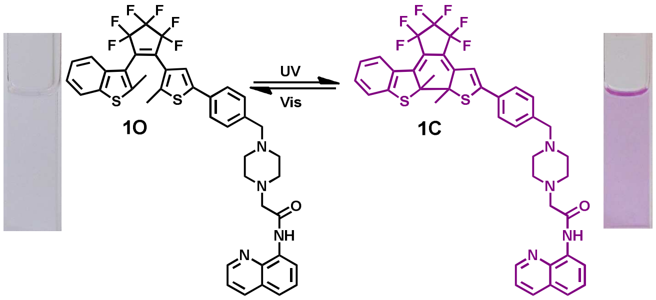

Fig. 1

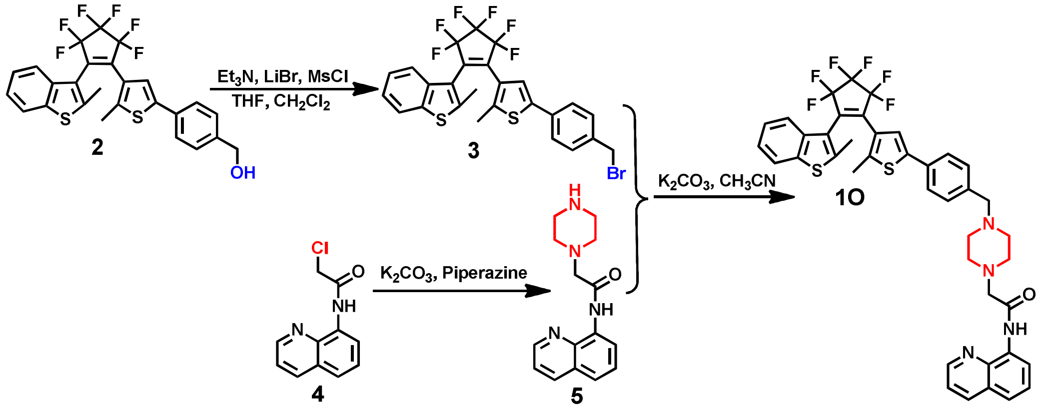

F
2
OH
Et3N, LiBr, MsCl
THF, CH2Cl2
3
Br
K2CO3, CH3CN
1O
Cl
O
NH
N
4
K2CO3, Piperazine
H
N
5
S

Fig. 2

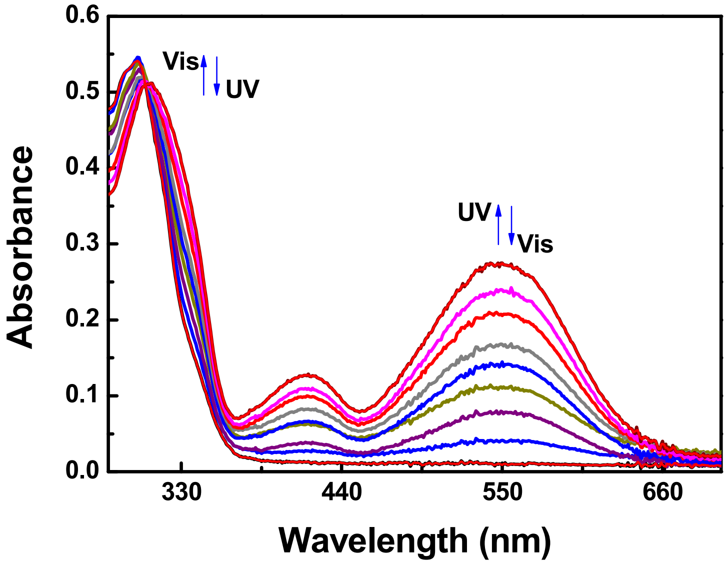
0.6
0.5
0.4
0.3
0.2
0.1
0.0
Absorbance
Vis
UV
UV
Vis
330
440
550
660
Wavelength (nm)

(A)

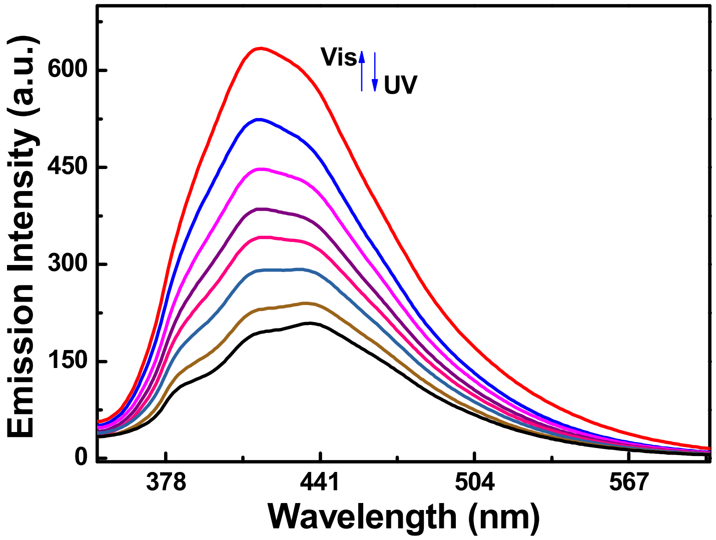
600
450
300
150
0
Emission Intensity (a.u.)
Vis
UV
378
441
504
567
Wavelength (nm)

(B)

Fig. 3

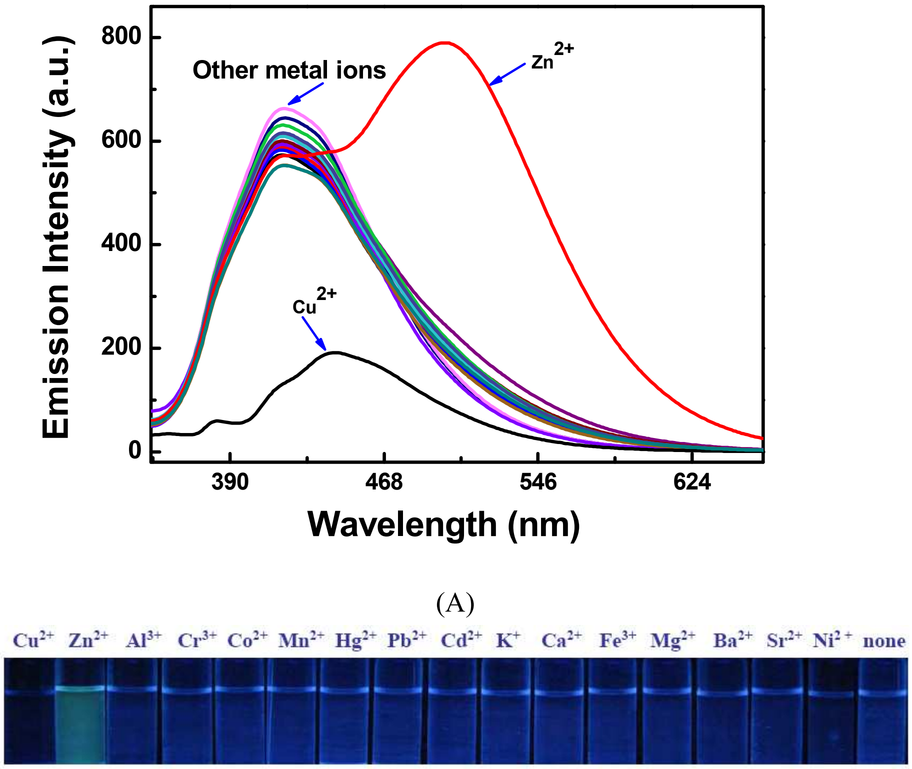
Emission Intensity (a.u.)
Wavelength (nm)
0
200
400
600
800
390
468
546
624
Other metal ions
Zn^{2+}
Cu^{2+}
Cu^{2+} Zn^{2+} Al^{3+} Cr^{3+} Co^{2+} Mn^{2+} Hg^{2+} Pb^{2+} Cd^{2+} K^{+} Ca^{2+} Fe^{3+} Mg^{2+} Ba^{2+} Sr^{2+} Ni^{2+} none

(A)

(B)

Fig. 4

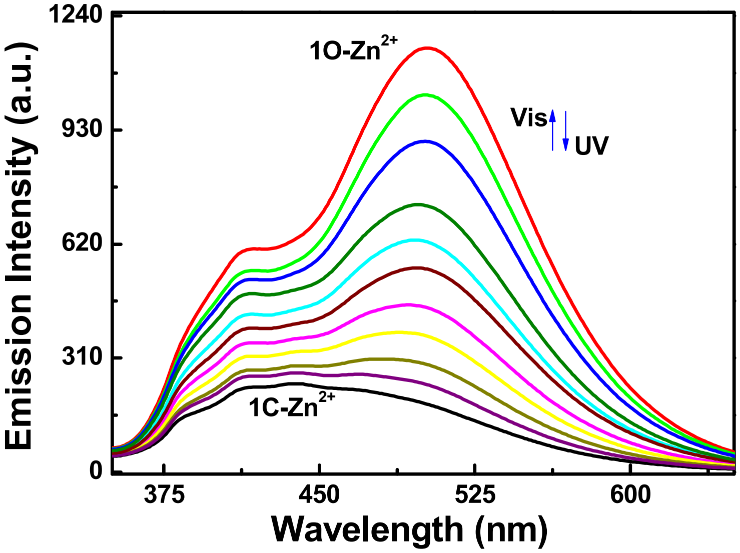
1240
930
620
310
0
375
450
525
600
Emission Intensity (a.u.)
Wavelength (nm)
1O-Zn2+
Vis
UV
1C-Zn2+

(A)

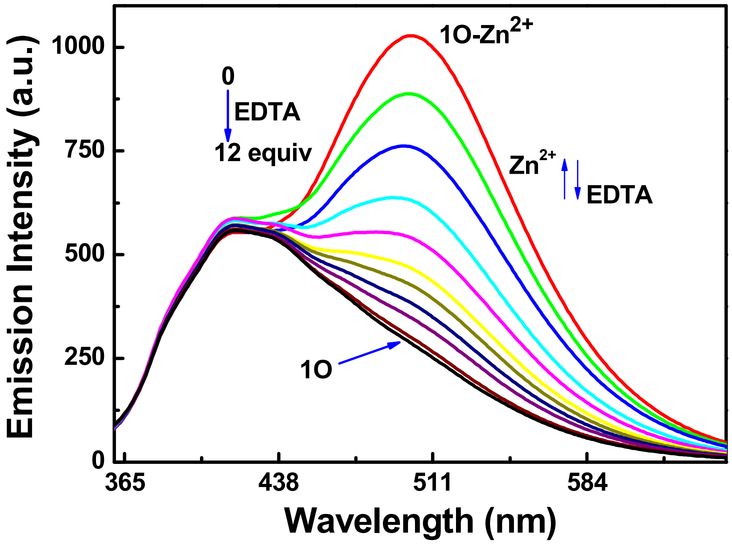
1000
750
500
250
0
365
438
511
584
Emission Intensity (a.u.)
Wavelength (nm)
1O-Zn2+
0
EDTA
12 equiv
Zn2+
EDTA
1O

(B)

Fig. 5

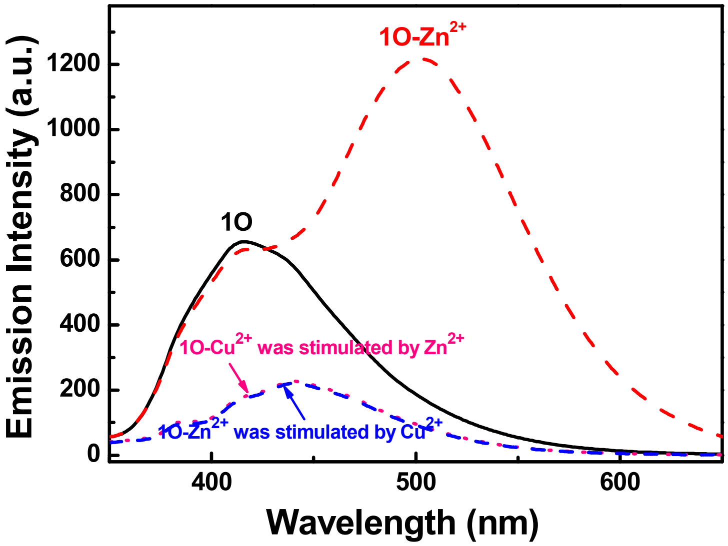
1O-Zn^{2+}
1O
1O-Cu^{2+} was stimulated by Zn^{2+}
1O-Zn^{2+} was stimulated by Cu^{2+}
Emission Intensity (a.u.)
0
200
400
600
800
1000
1200
400
500
600
Wavelength (nm)

(A)

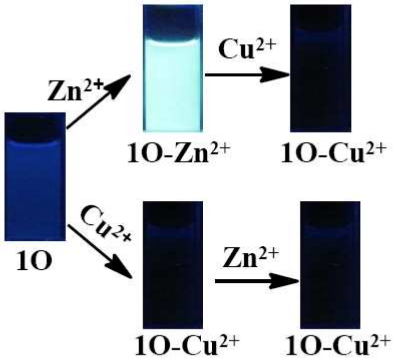
Zn^{2+}
Cu^{2+}
1O-Zn^{2+}
1O-Cu^{2+}
1O
Cu^{2+}
Zn^{2+}
1O-Cu^{2+}
1O-Cu^{2+}

(B)

Fig. 6

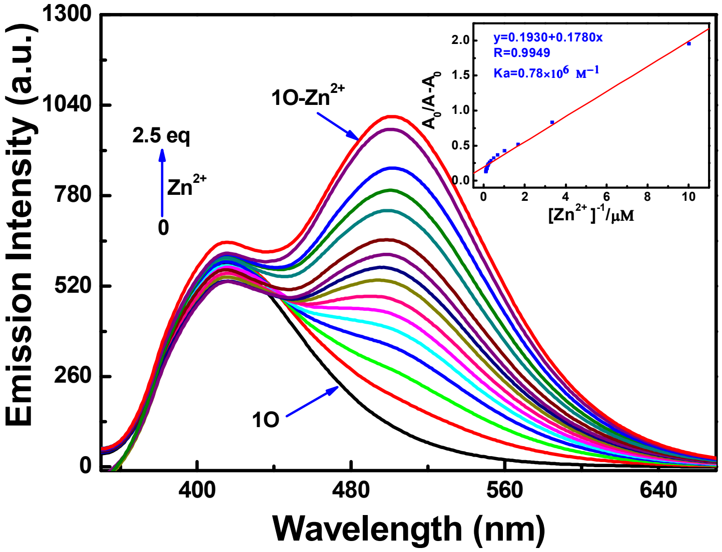

Emission Intensity (a.u.)
Wavelength (nm)
1300
1040
780
520
260
0
400
480
560
640
2.5 eq
Zn2+
0
1O-Zn2+
1O
y=0.1930+0.1780x
R=0.9949
Ka=0.78×10^6 M^-1
A0/A-A0
[Zn2+]^-1/μM
0.0
0.5
1.0
1.5
2.0
0
2
4
6
8
10

(A)

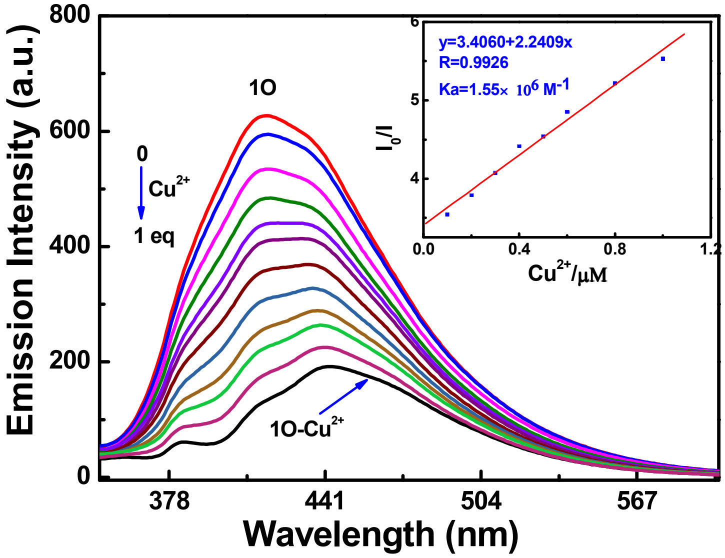

Emission Intensity (a.u.)
Wavelength (nm)
800
600
400
200
0
378
441
504
567
1O
0
Cu2+
1 eq
1O-Cu2+
y=3.4060+2.2409x
R=0.9926
Ka=1.55× 10^6 M^-1
I0/I
Cu2+/μM
6
5
4
0.0
0.4
0.8
1.2

(B)

Fig.7

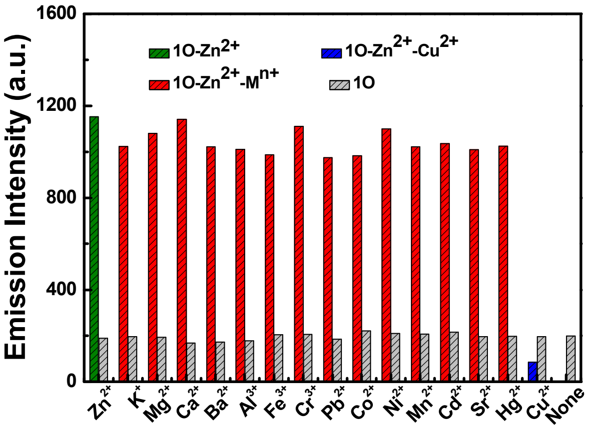
1O-Zn^{2+}
1O-Zn^{2+}-Cu^{2+}
1O-Zn^{2+}-M^{n+}
1O
Emission Intensity (a.u.)
1600
1200
800
400
0
Zn^{2+}
K^{+}
Mg^{2+}
Ca^{2+}
Ba^{2+}
Al^{3+}
Fe^{3+}
Cr^{3+}
Pb^{2+}
Co^{2+}
Ni^{2+}
Mn^{2+}
Cd^{2+}
Sr^{2+}
Hg^{2+}
Cu^{2+}
None

Fig. 8

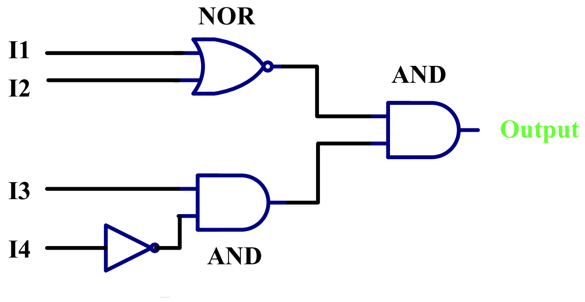

Fig. 9

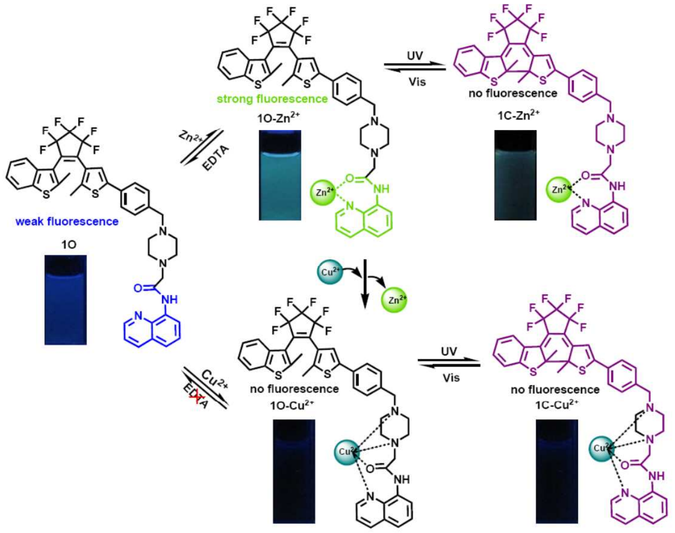

A new asymmetrical diarylethene with a piperazine-linked amidoquinoline unit was synthesized and its multi-controllable switching behaviors induced by light and chemical stimuli were investigated.